Supplement of

Technical note: Retrieval of the supercooled liquid fraction in mixed-phase clouds from Himawari-8 observations

Ziming Wang et al.

Correspondence to: Ziming Wang (Ziming.Wang@dlr.de)

S1 An analysis of cloud phase against temperature

Figure S1 illustrates the distribution of data point densities for each Himawari-8 cloud phase as a function of cloud top temperature (CTT). As expected, ice cloud tops predominate in colder temperatures, and water phases are prevalent in higher CTTs. The observed data are mostly consistent with the fact that temperatures below 233 K ice clouds primarily exist, and temperatures exceeding 273 K water clouds are observed (the horizontal blue and red lines). In the temperature range between these thresholds, water, ice and mixed-phase cloud tops are all observed, with the proportion of ice-containing cloud tops increasing towards colder temperatures (transitioning from mixed-phase, partly glaciated, to fully glaciated ice cloud tops). For CTT > 247 K, water phase prevails, between 246 K and 241 K, MPCs dominate, peaking at 241 K, and below CTTs of 240 K, the ice phase becomes the most frequent cloud type. Notably, the peak of CTTs for the ice phase exceeds 233 K, indicating a significant occurrence of liquid region ice clouds (Krämer et al., 2016).
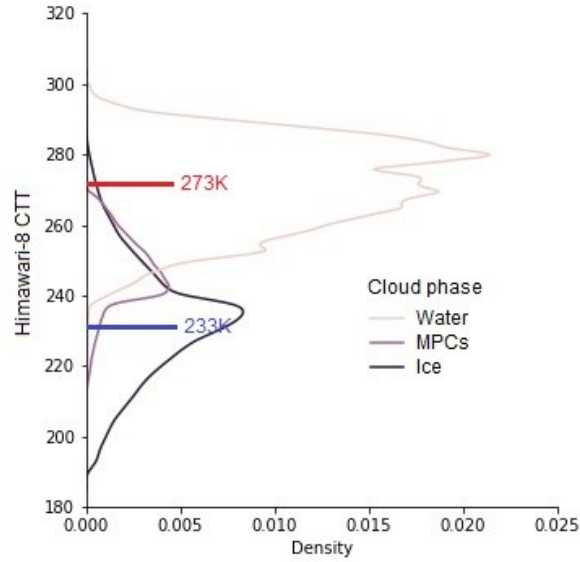
Figure S1: Densities of Himawari-8 cloud phase as a function of CTT. Blue and red lines mark the temperatures 233 K and 273 K.

S2 Establishment of the Random Forest based RTM emulator

20   We emulate the RTM model using the Random Forest (RF) (Ri et al., 2022) technique for predicting COT and CER of the assumed SCs and ice clouds, separately. The Mie scattering and droxtals ice crystals scattering database are incorporated in the atmospheric RTM RSTAR7. Based on the settings of look-up tables (LUTs) in the RTM in Table S1, we generate the corresponding four sets of training data. For the COT retrieval of either SCs and ice clouds, the inputs of the RF model are SZA, VZA, RAA, the satellite radiance at Band 0.64 μm, and albedo, the output is COT. The COT is derived if the real

25   Himawari-8 observations are available at the wavelength of 0.64 μm. For the CER estimation, the retrieved COT and the satellite radiance at Band 2.3 μm are added into the group of the input variables of the RF model, the output is CER. The CER is then inferred if the Himawari-8 observations at 2.3 μm are provided. The RTM emulators are validated with the prepared test datasets (randomly selected from the RTM simulations), and the high accuracy is shown in Fig. S2. We perform separate retrievals for cloud microphysical parameters for both SCs and ice cloud scenarios in Fig. S3.
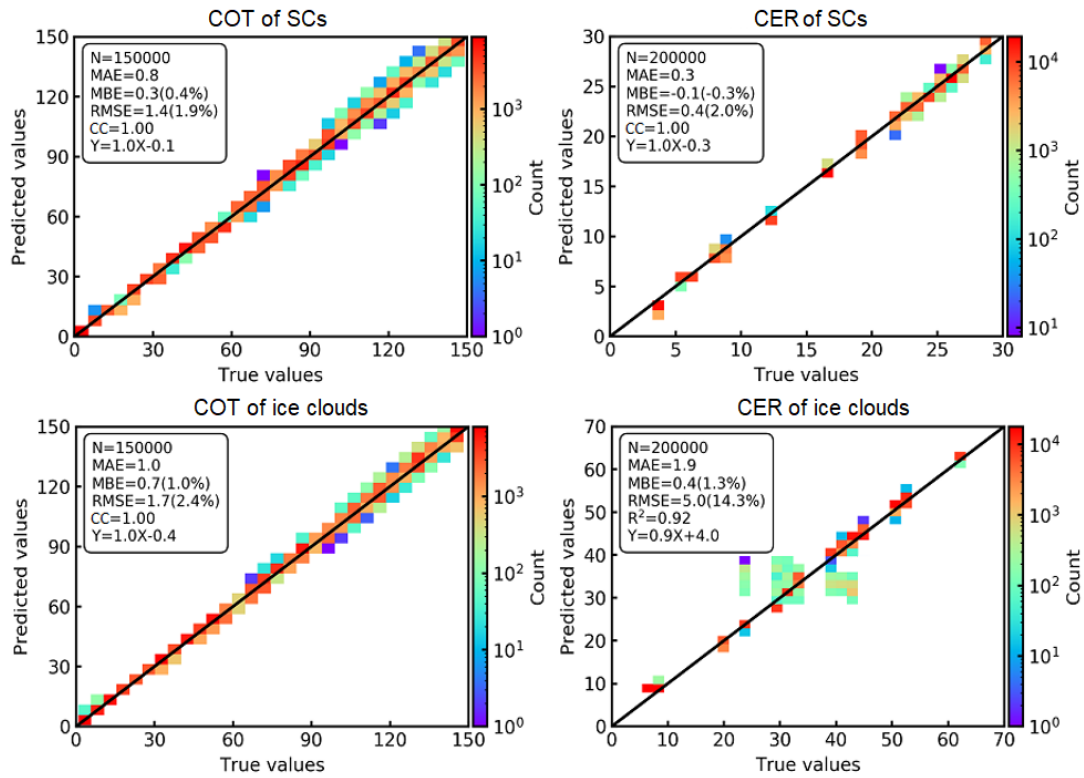
30

Figure S2: Validation of the RF based RTM emulators in the test dataset.
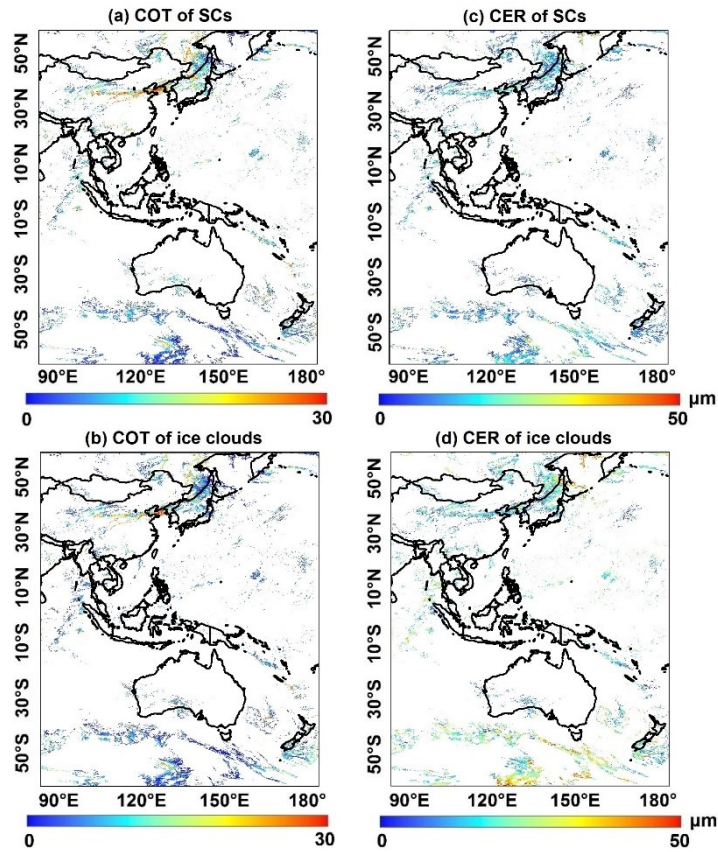
Figure S3: Retrieved microphysical properties of assumed SCs and ice clouds at 4:00 UTC on 28 August 2017 for MPC pixels. a. COT of SCs. b. COT of ice clouds. c. CER of SCs. d. CER of ice clouds.

Table S1: Grid points of the training data for the RTM emulator.

Variables	Range of values	Unit
SZA	0, 5, 10, 20, 30, 35, 40, 45, 50, 55, 60, 62, 64, 66, 68, 70, 72, 74, 76, 78, 80, 82, 84, 86, 88, 90	°
VZA	0, 5, 10, 20, 30, 35, 40, 45, 50, 55, 60, 65, 70, 75, 80	°
RAA	0, 10, 20, 30, 40, 50, 60, 70, 80, 90, 100, 110, 120, 130, 140, 150, 160, 170, 180	°
COT of the SLF	0.2, 0.5, 1, 2, 3, 4, 5, 6.5, 8, 10, 12, 14.5, 17, 18.5, 20, 21.5, 23, 25, 27, 29, 31, 33.5, 36, 38.5, 41, 44.25, 47.5, 50.75, 54, 58, 62, 66, 70, 75, 80, 85, 90, 95, 100, 105, 110, 115, 120, 130, 140, 150	-
CER of the SLF	3.5, 5.5, 6.5, 8.5, 9.5, 12.5, 17.5, 20, 22, 23, 24, 25, 26, 27, 28, 29.5	μm
COT of the IF	0.2, 0.5, 1, 2, 3, 4, 5, 8, 10, 12, 14.5, 17, 20, 23, 27, 31, 36, 41, 47.5, 54, 62, 70, 75, 80, 85, 90, 95, 100, 110, 120, 130, 140, 150	-
CER of the IF	7, 9, 20, 24, 30, 32, 34, 40, 42.5, 45, 47.5, 52.5, 55, 65	μm
Surface albedo	0.05, 0.1, 0.2, 0.3, 0.4, 0.5, 0.7, 1.0	-

Reference

Ri, X., Tana, G., Shi, C., Nakajima, T. Y., Shi, J., Zhao, J., Xu, J., Letu, H.: Cloud, atmospheric radiation and renewal energy Application (CARE) version 1.0 cloud top property product from himawari-8/AHI: Algorithm development and preliminary validation. IEEE T. Geosci. Remote, 60, 1–11. https://doi.org/10.1109/tgrs.2022.3172228, 2022.

Krämer, M., Rolf, C., Luebke, A., Afchine, A., Spelten, N., Costa, A., Meyer, J., Zöger, M., Smith, J., Herman, R. L., Buchholz, B., Ebert, V., Baumgardner, D., Borrmann, S., Klingebiel, M., and Avallone, L.: A microphysics guide to cirrus clouds – Part 1: Cirrus types, Atmos. Chem. Phys., 16, 3463–3483, https://doi.org/10.5194/acp-16-3463-2016, 2016.